

Quantum Chemical Study on the Circular Dichroism Spectra and Specific Rotation of Donor–Acceptor Cyclophanes

Tadashi Mori,^{*,†,‡} Yoshihisa Inoue,[†] and Stefan Grimme^{*,‡}

Department of Molecular Chemistry, Graduate School of Engineering, Osaka University, 2-1 Yamada-oka, Suita 565-0871, Japan, and Theoretische Organische Chemie, Organisch-Chemisches Institut der Universität Münster, Corrensstrasse 40, D-48149 Münster, Germany

Received: May 10, 2007

The structures of donor,acceptor-substituted cyclophanes were optimized by DFT and MP2 methods and compared with the X-ray crystallographic structures. The electronic circular dichroism (CD) spectra of these chiral cyclophanes were simulated by time dependent density functional theory (TD–DFT) with several functionals including different amounts of “exact” Hartree–Fock exchange. The experimental oscillator and rotatory strengths were best reproduced by the BH-LYP/TZV2P method. The specific rotation and vibrational circular dichroism (VCD) spectra were also calculated at the BH-LYP/aug-cc-pVDZ and B3-LYP/6-31G(d) levels, respectively, and compared with the experimental data. Better performance was obtained with the ECD, rather than the specific rotation or the VCD spectral calculations in view of the computation time and accuracy for the determination of absolute configuration (AC). The exciton coupling model can be applied only for the cyclophanes without CT-character. However, the split pattern found in the experiment does not appear to originate from a simple two-transition coupling, indicating that this method should be applied with caution to the AC determination. This conclusion was supported by the TD–DFT investigations of the transition moments and the roles of excited-state electronic configuration associated with these split bands. Cyclophanes with donor–acceptor interactions showed Cotton effects at the CT band and couplets at the 1L_a and 1L_b bands. Although the degree of charge transfer between the rings is very small, as revealed by a Mulliken–Hash analysis, the split Cotton effects are due to a large separation in energy of the donor and acceptor orbitals. The effect of the distance and angle between the donor and acceptor moieties in model (intermolecular) CT complexes on the calculated CD spectra was also studied and compared with those obtained for various paracyclophanes.

1. Introduction

A considerable interest has been paid over the years to a variety of substituted cyclophanes¹ because of their planar chirality, which is known to behave quite differently from conventional point chirality in asymmetric reactions, catalysis, and host–guest interactions.² Since the locally excited 1L_a and 1L_b transitions of the two aromatic rings in chiral cyclophanes are strongly coupled, the absolute configurations (AC) of some cyclophanes have been determined by simply applying the exciton chirality method.^{3,4} The electronic transition moments of two chromophores positioned at appropriate distance and orientation in a chiral environment couple to each other, resulting in a splitting of the energy levels, which is most clearly displayed by a bisignate coupled circular dichroism (CD) spectrum. From the sign of the couplet, the AC is usually assigned without any difficulty. However, we have recently shown that the exciton chirality method does not give the correct AC for some donor-acceptor cyclophanes, i.e., 4,7-dicyano-12,-15-dimethoxy[2.2]paracyclophanes.⁵ Although we tentatively assigned the origin of this inconsistency to the significantly distorted transition moments due to the intramolecular charge-transfer (CT) interactions and/or deformation of the aromatic

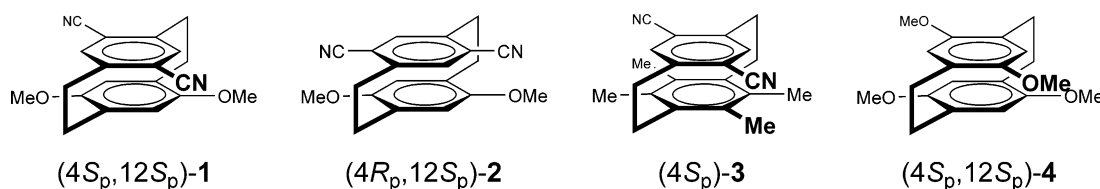
rings, a full analysis of the chiroptical properties of such donor–acceptor cyclophanes remains to be elucidated.

In the present study, we performed time-dependent density functional theory (TD–DFT) calculations⁶ and analyzed in detail the experimental and simulated circular dichroism (CD) spectra of representative CT paracyclophanes (Chart 1), i.e., (4*S*_p,12*S*_p)- and (4*R*_p,12*S*_p)-4,7-dicyano-12,15-dimethoxy[2.2]paracyclophanes (**1** and **2**) and (4*S*_p)-4,7-dicyano-12,13,15,16-tetramethyl[2.2]-paracyclophane (**3**). The results are compared with those obtained for a non-CT cyclophane, i.e., (4*S*_p,12*S*_p)-4,7,12,15-tetramethoxy[2.2]paracyclophane (**4**) to reveal that the exciton chirality theory cannot be applied to the donor–acceptor cyclophanes since the apparent couplet observed in the experimental spectrum turned out to be a mere overlap of the individual Cotton effects with the opposite signs. Moreover, the application of the conventional exciton chirality theory to non-CT cyclophanes seems controversial, since complicated cancellations between the transitions are generally involved, although the excitons are indeed coupled in such cyclophanes. We also discuss other chiroptical properties such as specific optical rotations and vibrational CD spectra of these molecules to assess the performance of the AC determination using CD spectra. Finally, we will describe the influence of inter-ring angle and distance on the CD spectrum of an intermolecular CT model complex. This demonstrates that CT paracyclophanes are

* To whom correspondence should be addressed. Fax: +81-6-6879-7923. E-mail: tmori@chem.eng.osaka-u.ac.jp.

[†] Osaka University.

[‡] Universität Münster.

CHART 1: Chiral Donor–Acceptor and Related Cyclophanes

excellent systems for closely understanding the intermolecular donor–acceptor interactions in a larger context.

2. Computational Details

All calculations were performed on Linux-PCs using the TURBOMOLE 5.6 program suite.⁷ The resolution of identity (RI) approximation^{8,9} was employed in all DFT/B-LYP calculations, and the corresponding auxiliary basis sets were taken from the TURBOMOLE basis set library. The program modules *escf*¹⁰ and *ricc2*⁹ have been used in the TD–DFT and coupled-cluster (CC2) response treatments. All conformers of the donor–acceptor cyclophanes and relevant donor and acceptor molecules were fully optimized at the dispersion corrected DFT–D/B-LYP level¹¹ without symmetry constraints (C_1 symmetry), using an AO basis set of valence triple- ζ quality with two sets of polarization functions (2d2p, denoted as TZV2P; in standard notation: H, [3s2p], C/N/O, [5s3p2d]) with numerical quadrature multiple grid (m4 in TURBOMOLE terminology). Subsequent single-point energy calculations were performed with the spin-component-scaled (SCS)-MP2 method¹² employing basis-sets of triple- ζ quality (TZVPP:¹³ i.e., added f and d functions on non-hydrogen and hydrogen atoms, respectively, compared to TZV2P) and that was used for the final Boltzmann distribution between the conformers. For most of the stable conformers, structures were also optimized both with HF/SV(P)¹⁴ and MP2/TZVPP methods. All excited-state calculations have been performed at the ground-state geometries. The results thus obtained correspond to the vertical transitions, and the excitation energies can be approximately identified as the band maxima in the experimental spectra. More robust length-gauge representations were used throughout this study for all calculations of rotatory strengths, although differences between length and velocity-gauge representations are found to be very small. The CD (and UV–vis) spectra were simulated with the time-dependent density functional theory (TD–DFT) method with several functionals including different amounts of exact exchange and using the same TZV2P basis-set. The CD spectra were simulated by overlapping Gaussian functions for each transition where the width of the band at 1/e height is fixed at 0.4 eV. See ref 15 for more theoretical details of the simulation of the CD spectra. The spectrum of **3** was also calculated by the RI-CC2 method^{9,16} with a smaller SVP basis-set. Unfortunately, due to technical reasons we could not obtain converged results with larger basis sets mainly due to the size of the molecule. The specific rotations were calculated at BH-LYP/aug-cc-pVDZ and B3-LYP/aug-cc-pVDZ levels for the same optimized structures. The theoretical VCD (and IR absorption) spectra were simulated at the B3-LYP/6-31G(d) level on Gaussian 03 Program suite¹⁷ with Lorentzian band shapes of 20 cm^{-1} full width at half-mean and applying a scaling factor of 0.96 for the computed harmonic frequencies.¹⁸

3. Results and Discussion

Geometrical Optimization of Donor–Acceptor Cyclophanes. Possessing a rigid structure that can force two aromatic

planes to face each other, [2.2]cyclophanes, in particular [2.2]-paracyclophanes,¹ have played a significant role in structural/mechanistic studies over the years and served as valuable probes for understanding the interplay of aromaticity vs strain, transannular interactions, and substituent effects.¹⁹ The accurate calculation of cyclophane's molecular geometries by quantum chemical methods is quite challenging. Simple DFT methods underestimate or neglect the dispersive interactions (π – π correlations) between the two aromatic rings leading to too long inter-ring distances, while the standard MP2 method, on the contrary, overestimates such dispersive effects.²⁰ Therefore, the geometries of the present (donor–acceptor) paracyclophane molecules were investigated using the DFT–D–B-LYP method. We have recently developed an empirical correction scheme for efficient DFT calculations (mainly geometry optimization) by adding pairwise $-C_6/R^6$ potentials to describe the van der Waals interactions (DFT–D method). This dispersion corrected DFT is a very efficient practical alternative to the electron correlated methods such as MP2 or CCSD(T) and has been successfully applied to weakly bound intermolecular complexes²¹ and also to a relatively large host–guest (tweezers) molecules.²² (For an overview, see ref 23.) The method is as efficient as conventional DFT and the calculated energies and geometries are fairly comparable to those obtained by the improved SCS-MP2 method.²⁴

All possible conformers of each of **1–4** were fully optimized without any symmetry constraints. We carefully considered the well-known conformational problem that appears as $D_2 \leftrightarrow D_{2h}$ symmetry breaking problem (double-minimum potential) in the parent paracyclophane system.^{20,25} It turned out that, in the equilibrium structures, two methylene bridges are slightly de-tilted pointing to such a direction that is open to avoid the steric repulsion between adjacent groups and the methylene protons. The conformers with oppositely tilted methylenes are not local minima and optimizations always converged to the initial (thus tilted to the less-hindered) structures. Figure 1 illustrates all of the DFT–D optimized structures of paracyclophanes **1–4**. In all cyclophanes, the relative energy consistently increases with increasing number of perpendicular methoxy group(s). The conformers are labeled from **a** to **c** (or to **g** for **4**) in the order of increasing relative energy. For the most stable conformers of **1a**, **2a**, **3**, and **4a**, optimizations with the standard MP2 and uncorrelated HF method were also carried out for a comparison purpose. The characteristic structural parameters (Chart 2) such as mean plane distance and deformation angles are compared with those of the X-ray crystallographic structures⁵ (where available), and the results are summarized in Table 1.

The energetically most favored conformers of **1** and **2** are essentially C_2 -symmetric as was the case in the parent cyclophane. All of the attached methoxy groups are in the plane of the aromatic ring, in good agreement with the X-ray crystallographic structures.⁵ Inter-plane distances are slightly overestimated in the DFT–D calculations, but the deviations from the X-ray structures are less than 1 pm. The deformation angles (α and β) also nicely agree with the X-ray structure values. In

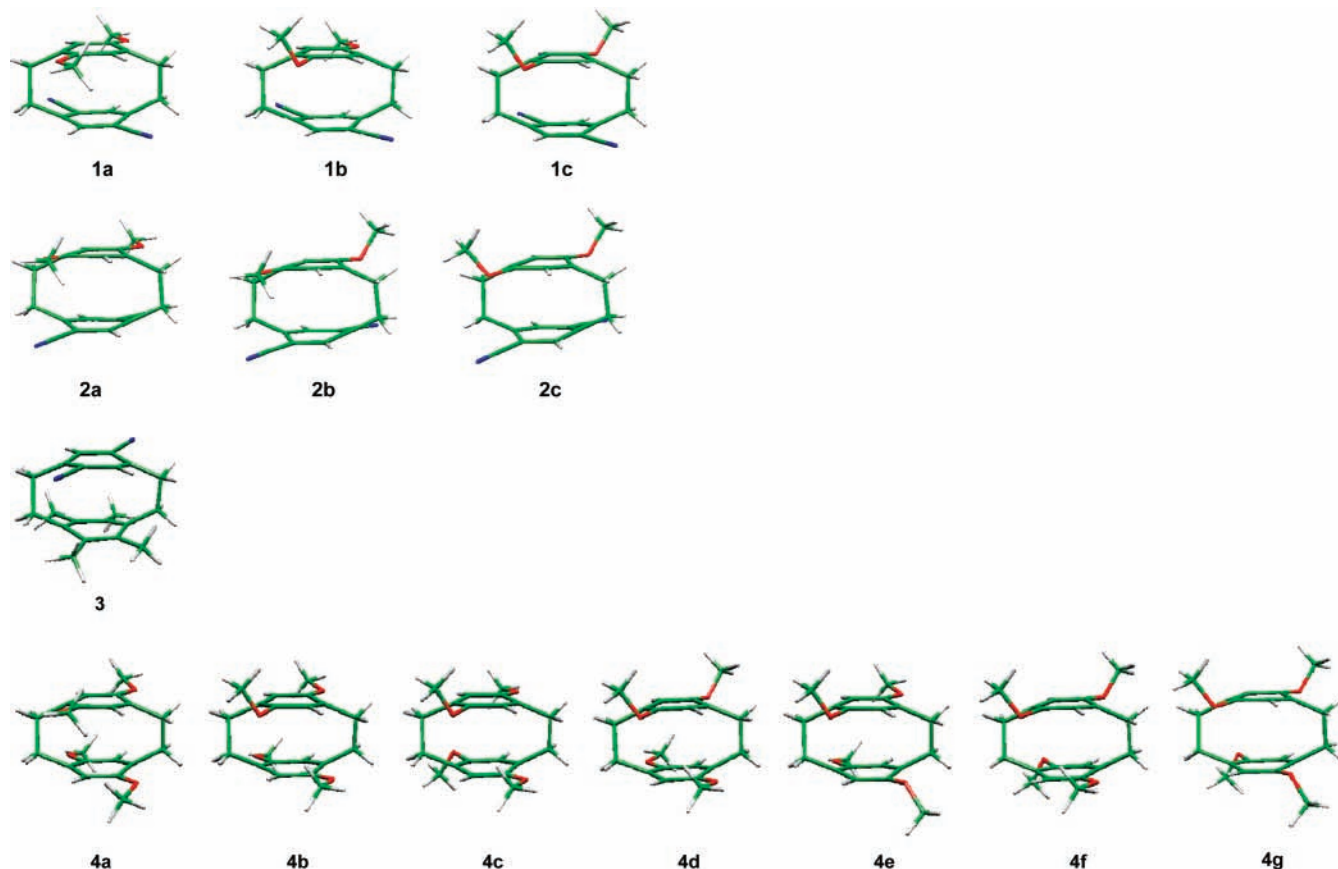
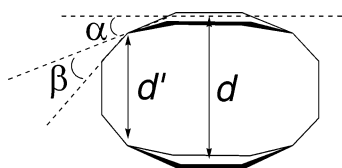


Figure 1. DFT-D optimized structures of three conformers of **1** and **2**, most stable conformer of **3**, and seven conformers of **4**.

CHART 2: Important Structural Parameters of Cyclophanes



contrast, MP2 optimization yielded poorer results; thus, the inter-plane distances are underestimated in **1** and the deformation angles are much larger. The relatively good agreement of the inter-plane distance in **2** would be incidental, since the deformation angles are considerably deviated. The tilt angles of the ethylene linker against the aromatic planes are known to be very sensitive to the conditions of measurement. No calculated values obtained by any of the above methods are very satisfactory. Thus the overall accuracy of the calculated structures decreases in the order DFT-D > MP2 \gg HF. This conclusion is reinforced by the fact that the CD spectra (as well as the other chiroptical properties) calculated on the basis of the DFT-D structures are in excellent agreement with the experimental results (vide infra); for additional examples of similarly good performance of the DFT-D method, see Figure S1 of the Supporting Information. Compared with **1** and **2**, **3** has slightly longer inter-ring and inter-bridgehead distances, due to the steric hindrance of the four methyl groups attached to the aromatic ring, thus exhibiting a larger degree of deformation. The structural parameters of **4** are quite similar to those of **1** and **2**, indicating that the effect of donor-acceptor interactions in CT cyclophanes on the geometries is not very large (vide infra).

Calculation of Optical Rotation. The present-day TD-DFT implementation for chiroptical property calculations such as

optical rotations (OR)²⁶ and CD spectra^{27,28} have recently been applied with success to the assignment of the AC of chiral organic molecules. Accordingly, we also performed the calculation of OR for the cyclophanes **1–4** with BH-LYP and B3-LYP functionals using the Dunning's²⁹ aug-cc-pVDZ basis-sets. The SCS-MP2/TZVPP energies were used to compute the Boltzmann distributions of the conformers for each paracyclophane.²⁴ For the most stable conformers of **1** and **2**, the aug-cc-pVTZ sets were employed to check the basis-set incompleteness effects. The results are summarized in Table 2. With the popular B3-LYP functional, the calculated $[\alpha]_D$ values are rather disappointing and this approach even fails to provide the correct signs for both **1** and **2**. This disappointing result may be attributed to a significant underestimation of the excitation energy of the charge-transfer transitions³⁰ that appear too close in wavelength to the sodium D-line (589.3 nm) and hence improperly influences the optical rotation owing to the small energy denominators. These problems were solved at least in part by including a larger content of exact Hartree-Fock exchange in the functional. Thus, the calculated $[\alpha]_D$ values with BH-LYP functional (50% exact exchange) are more reliable in the present cases (as shown in the CD calculation, vide infra) and the AC of **1** and **2** are now correctly predicted by theory. However, as judged from the large discrepancy between the aug-cc-pVTZ and aug-cc-pVDZ values for **1**, the magnitude of the ORs is not accurately calculated with this small basis-set. Most of the calculations were done with the DFT-D optimized geometries, but the calculations were also performed for the MP2-optimized geometries with the same aug-cc-pVDZ basis-set for a comparison purpose. No ORs calculated at the BH-LYP/aug-cc-pVDZ level for the MP2-optimized cyclophanes were satisfactory, despite that the value for **1** was coincidentally acceptable. This might be, at least in part, due to the basis-set

TABLE 1: Comparison of X-ray Crystallographic and Calculated Structures of Most Stable Conformers of **1–4**^a

	1		2		3		4								
	X-ray	HF/SV(P)	BLYP/TZV2P	MP2/TZV2P	X-ray	HF/SV(P)	BLYP/TZV2P	MP2/TZV2P	HF/SV(P)	BLYP/TZV2P	MP2/TZV2P	MP2/TZVPP			
energy, E_h		-1025	-1032	-1030		-1025	-1032	-1030		-953	-961	-959	-1069	-1077	-1075
mean plane distance, d , Å		0.5700	0.8733	0.8306		0.5651	0.8694	.8254		.9806	.0039	.0608	.8184	.1134	.3134
bridged head distance, d' , Å		3.132	3.126	2.881		3.154	3.158	3.006		3.240	3.204	3.056	3.116	3.139	2.973
α value at the donor side, deg		2.759	2.808	2.710		2.812	2.826	2.720		2.846	2.834	2.731	2.813	2.836	2.717
β value at the donor side, deg		11.3	11.9	9.5		12.2	12.1	10.5		16.9	15.8	14.3	12.3	12.2	10.6
α value at the acceptor side, deg		12.8	12.2	13.2		12.0	12.2	12.8		9.0	8.6	10.2	12.3	12.7	12.8
β value at the acceptor side, deg		12.5	13.8	11.5		13.8	14.0	12.8		15.0	13.9	12.6	12.3	12.7	12.8
tilt angle of the linker, deg		10.6	10.8	11.4		9.6	10.2	10.6		10.5	10.2	11.1	18.3	16.6	17.2
dihedral angle of methoxy group, deg		9.6	12.6	14.5		11.8	12.7	16.8		18.6	9.1	20.0	25.2	15.9	18.4
		7.5	6.0	8.5		9.6	8.6	12.3							

^a Optimization was performed at the HF/SV(P), DFT-D-B-LYP/TZV2P, or RI-MP2/TZVPP levels. See text for more details on the calculations. See also Chart 2 for the structural parameters of the cyclophanes.

incompleteness effects for those structures. Regardless, one must be cautious in using the calculated specific rotations for AC determination, since they are so sensitive to the structure employed and may give values with the opposite sign for compounds with unusual structural features (at least such as paracyclophanes).

Calculation of the VCD Spectra. Recent instrumental and theoretical advances in vibrational circular dichroism (VCD) spectroscopy have enabled the elucidation of conformations of chiral organic and biological molecules in solution,^{18,31} and also the AC determination of relatively rigid chiral molecules through the combined use of DFT calculations and a sophisticated FT-VCD instrument.³² We also performed the conformer-population-weighted VCD calculations for the present paracyclophane systems, although the AC assignment of the most abundant conformers of **1** and **2** was recently done by using the combined DFT and VCD studies.⁵ Figure 2 (left) shows the comparison of the calculated and the experimental VCD spectra of cyclophanes **1**, **2**, and **4**. Unfortunately, we were unable to obtain an enough amount of enantiopure sample of **3** for the VCD measurement, due to the poorer HPLC separation and the low solubility of this compound (See Table S1 in Supporting Information for the detailed conditions of enantiomer separation). The CD spectrum was calculated at the B3-LYP/6-31G-(d) level for each conformer that is geometrically optimized at the same level. The spectra obtained for all possible conformers are averaged over the SCS-MP2 energy-based Boltzmann populations. Figure 2 (right) shows the VCD spectra calculated for all possible conformers. Although the calculated and observed VCD spectra apparently resemble each other, a closer look reveals several mismatches.

Briefly, the sign of the 1600 cm^{-1} peak, assignable to C=C stretch, was correctly reproduced for all of the cyclophanes, but the split pattern in the simulated spectra of **1** and **2** was not clearly observed experimentally. More importantly, the signal-(s) of the 1400 cm^{-1} peak, assigned to C-H scissoring, were not reproduced very well. This is reasonable if we assume the dynamic conformational variations of the ethylene linker of the cyclophanes in solution. Furthermore, there are several missing bands (e.g., at 1300 cm^{-1}) if one compares the calculated and the experimental VCD spectra. We may conclude therefore that the VCD-based AC determination (of cyclophanes) is not reliable, especially when the structure is not very rigid and the molecule has many conformational variations. In such a case, the concurrent use of other AC determination method(s) is highly recommended.

Calculation of the CD Spectra. *A. Effect of Functionals on the Calculated CD Spectra of Donor-Acceptor Cyclophanes 1 and 2.* Although the calculation of rotatory dispersion is more general (requiring no particular chromophore), it has only recently been recognized³³ that the combined use of the circular dichroisms and optical rotations (or dispersions) is essential for an accurate AC determination, especially when the $[\alpha]_D$ value is not very large.³⁴ We have recently reported that the use of Becke's half-and-half (BH-LYP) functional³⁵ is of particular importance in the evaluation of the CD spectra of the donor-acceptor dyad system.³⁶ Here we compare the effect of the chosen density functional with different degree of exact exchange mixing on the performance of the CD spectral calculation of the donor-acceptor cyclophanes **1** and **2**. The calculated CD spectra were obtained by Boltzmann averaging of the calculated oscillator and rotatory strengths for each conformer with different functionals and with the TZV2P basis-sets (for individual calculated CD spectra of the conformers,

TABLE 2: SCS-MP2 Relative Energies, Boltzmann Populations of Conformers Derived Therefrom and the Calculated Specific Rotations of 1–4^a

	relative energy, kcal/mol	% population	optical rotations			experimental
			BH-LYP/aug-cc-pVDZ	BH-LYP/aug-cc-pVTZ	B3-LYP/aug-cc-pVDZ	
1a	≡0	89.0	−24.9 (−25.2 ^b)	−114.5	+100.8	
1b	2.16	10.3	−70.8		+2.3	
1c	4.89	0.7	−50.1 −29.8 ^c		+0.9 +90.0 ^c	−21.7
2a	≡0	95.2	−5.4 (+26.9 ^b)	−6.3	+109.5	
2b	3.02	4.7	−157.3		−161.7	
2c	6.66	0.1	−252.7 −12.8 ^c		−299.7 +96.4 ^c	−89.7
3			−101.0 (+419.0 ^b)		−119.2	−20.2
4a	≡0	32.8	−91.4 (+178.0 ^b)			
4b	0.23	26.0	−111.6			
4c	0.24	25.7	−150.0			
4d	1.03	11.7	−92.8			
4e	2.61	2.4	n.d. ^d			
4f	3.27	1.3	n.d. ^d			
4g	6.06	0.1	n.d. ^d −112.7 ^e			−154.0

^a Specific rotations were calculated for the enantiomers shown in Chart 1. ^b Calculation was performed on the MP2-optimized structures. ^c Calculated specific rotation corrected for the conformer population. ^d Not determined. ^e Calculated specific rotation corrected for the population of four most contributing conformers (**4a–4d**).

see Figure S2 in Supporting Information; see also Figure S3 in Supporting Information for bar-representation of the spectra of the most stable conformers). For **4**, the most contributing four conformers (of >10% population) are considered in the CD calculations.

In our calculations, the TD–HF method (100% exact exchange) as well as TD–DFT methods with three different functionals (BH-LYP, B3-LYP, and B-LYP) with systematically varying fraction of exact exchange in the functional (50, 20, and 0%, respectively) have been employed to monitor the deviation of the excitation energies and the rotatory strengths of the charge transfer, ¹L_b, and ¹L_a transitions. The results of the simulations for cyclophanes **1** and **2** are shown in Figure 3. In the TD–HF approach, a systematic overestimation of all excitation energies was found as pointed out previously,³⁷ and thus the entire spectrum was shifted to the red by 0.4 eV for a better agreement with experiment. Note that charge transfer states in the TD–HF calculations were not found for both **1** and **2**. As the fraction of HF exchange (BH-LYP and B3-LYP) was decreased, the excitation energy was lowered and the required shift was decreased to about 0.2 eV. In the case of the B-LYP functional, even a 0.2 eV blue-shift was required. For **1**, all three functionals gave relatively satisfactory agreement with the experimental results. In contrast, the spectra of **2** are more complicated, showing a complex splitting pattern (for the details of the experimental CD spectra, see Table S2 in Supporting Information). The CD spectra calculated for this compound were less satisfactory than those for the staggered cyclophane **1**, especially with the B-LYP functional. With B3-LYP, significant underestimation of the charge-transfer excitation energy is observed (as reported previously³⁰ for model compounds), and the overall agreement with the experiment is not good. The best result was obtained with the BH-LYP functional.³⁸ Judging from the almost perfect agreement of the calculated with the experimental CD spectra of both **1** and **2**, we may conclude that the calculation of the CD spectra on the donor–acceptor paracyclophanes at the BH-LYP/TZV2P level can unambiguously determine the absolute configuration of the molecules.

B. CD Spectrum Calculations for Related Cyclophanes with Less-Polarizing Donor Groups (3) and without CT Interactions (4). The calculation of the CD spectra of **3** is much more

challenging, since the direction of the electronic and magnetic transition moments in the donor are not very explicitly defined as all of the substituents are quite similar (methyl or methylene) in the donor moiety. It is consequently not possible to apply the conventional exciton chirality theory, which requires quite accurate knowledge about the orientation of the relevant transition moments. In addition, the DFT–VCD method was not applicable to **3** due to the low solubility and the difficulty of preparing large amounts of enantiopure samples as a consequence of the poor chiral HPLC separation. Thus, the quantum chemical computation is practically the only method available for the determination of the AC of this cyclophane. As shown in Figure 4 (left) (see Figure S3 in the Supporting Information for a bar-representation), the calculated CD spectrum is in reasonable agreement with the experimental spectrum, especially in the ¹L_a transition region (~250 nm). The sign of the Cotton effect of the CT transition (~360 nm) is also correctly predicted by the theory, although some deviation (slight enhancement) in the relative rotatory strength is observed. The origin of the discrepancy in the ¹L_b transition regions is not completely clear at present, but presumably attributable to the more multireference character of the transition. The spectrum is expected to be better reproduced at a higher level of theory such as CC2 or DFT/MRCI. The RI-CC2 calculation with slightly smaller basis-set (SVP) afforded very good theoretical CD spectrum (Figure 4, middle). Accordingly, (+)-**3** can be safely assigned to the (4S_p)-enantiomer. The underestimation of the CT excitation energies with the B3-LYP functional was also observed for this compound and this functional more or less failed to reproduce the entire experimental spectrum. It turned out that the use of the TZV2P instead of the TZV2P basis-set and/or C₂ symmetry does not affect the overall CD spectral pattern, at least in the examined wavelength range. Figure S3 in Supporting Information compares the effect of functional and basis-set on the calculated CD spectra of **3** with and without C₂ symmetry constraints in detail.

The calculation of the CD spectra of the cyclophanes without any donor–acceptor interaction (**4**) can also be successfully performed at the same level of theory (BH-LYP/TZV2P) as shown in Figure 4, right (see Figure S3 in Supporting Informa-

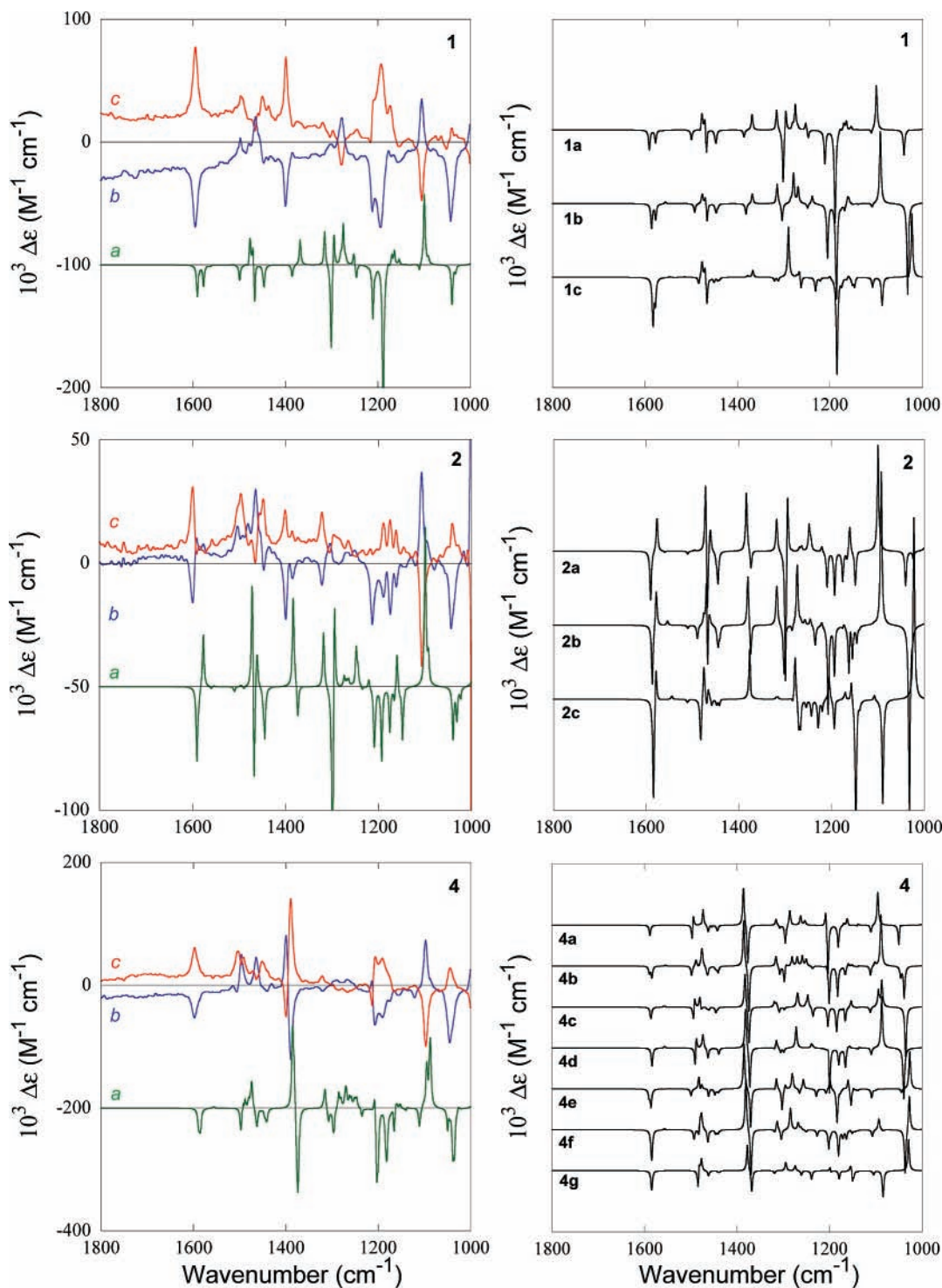


Figure 2. Left: (a) Conformer-averaged VCD spectra of $(4S_p, 12S_p)$ -**1**, $(4R_p, 12S_p)$ -**2**, and $(4S_p, 12S_p)$ -**4** calculated at B3LYP/6-31G(d) level. The vertical axis is shifted for clarity. (b and c) Experimental VCD spectra for (–)- and (+)-isomers, respectively. Right: Calculated VCD spectra for each conformer. Calculated VCD spectra were scaled to 1/2.

tion for a bar-representation of the spectra of conformer **4a**). For this compound, four out of seven conformers contribute to the overall CD spectrum (vide supra), which are averaged by SCS-MP2 energy-based populations (for individual CD spectra of the conformer, see Figure S2 in Supporting Information). Accordingly, the calculated $(4S_p, 12S_p)$ -isomer can be assigned to the (–)-isomer, which also agrees with the result from the VCD experiment.

Excited State Analysis and Molecular Orbitals Associated with the Transitions. Details of the results on the excited-state analysis such as configuration contributions for all paracyclo-

phanes **1–4** are shown in Table S3 in the Supporting Information. We will, hence, concentrate on the excited-state properties of cyclophanes **1** and **4** as typical examples (Figure 5). The bar-representation of the transitions in **1a**, and their relative contribution, are shown in Figure 5 (left). As clearly shown, no exciton coupling is involved in any of the observed bands. The apparent couplet around 300 nm, for instance, turned out to be an overlap of the oppositely signed independent $\pi-\pi^*$ transitions of the acceptor (**3**) and the $\pi-\pi^*$ transitions of donor with some contribution from the donor-to-acceptor transitions (**4**). Thus, the contribution of the relevant transitions can be

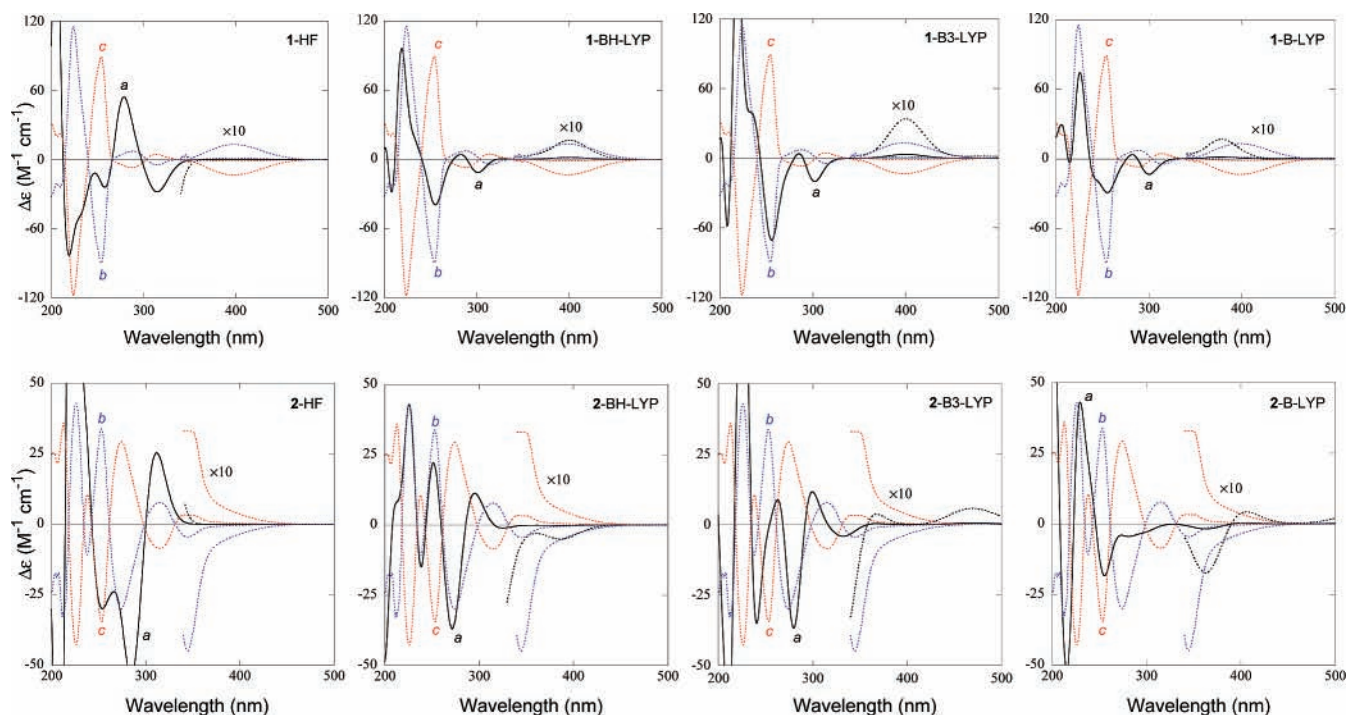


Figure 3. Influence of the density functional on the calculated CD spectra of **1** (top) and **2** (bottom). (a) Calculated spectra were obtained by averaging three conformers of $(4S_p,12S_p)$ -**1** or $(4R_p,12S_p)$ -**2**. (b and c) Experimental CD spectra for (–)- and (+)-isomers. From left to right: HF with 0.4 eV red-shift, BH-LYP with 0.2 eV red-shift, B3-LYP with 0.2 eV red-shift, and B-LYP with 0.2 eV blue-shift of calculated excitation energies.

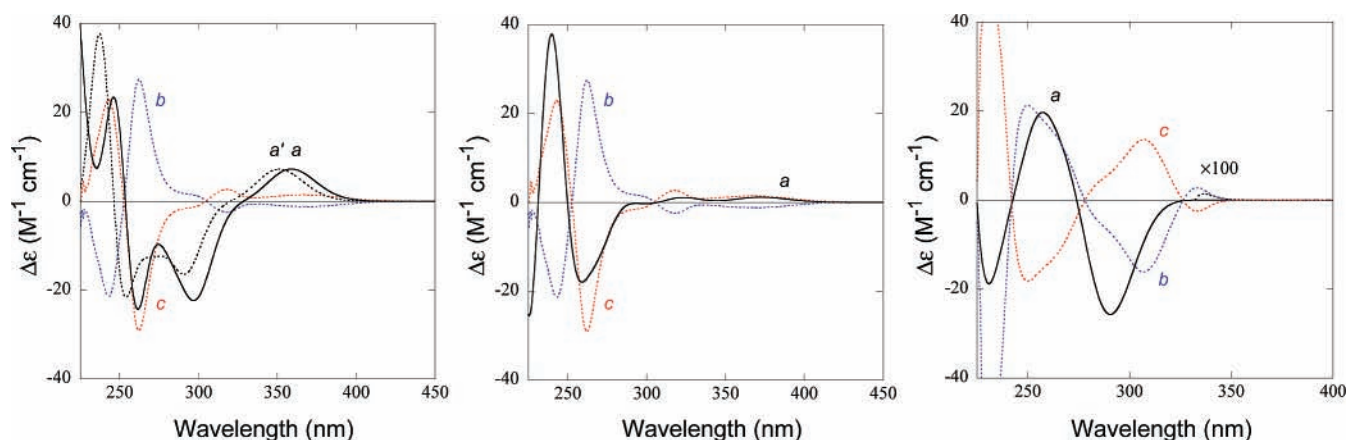


Figure 4. Left: Simulated CD spectra at BH-LYP/TZV2P (a) and SVP (a') levels of $(4S_p)$ -**3** with 0.2 eV red-shift with reduced intensity (one-half). Middle: Simulated CD spectra at RI-CC2/SVP level of $(4S_p)$ -**3** with 0.5 eV red-shift with reduced intensity (one-fifth). Right: Simulated CD spectra at BH-LYP level by averaging the four major conformers of $(4S_p,12S_p)$ -**4** with 0.4 eV red-shift. (b and c) Experimental CD spectra for (–)- and (+)-isomers.

assigned in the order of decreasing transition energy as donor–acceptor (CT), CT, π – π^* of acceptor, CT + π – π^* of donor, CT + π – π^* of donor, and π – π^* of acceptor, and so forth, respectively, as labeled in Figure 5 (left). Therefore, the observed CD spectra can be analyzed as a simple overlap of the Cotton effects of pure π – π^* transitions in the donor part and/or the acceptor part, accompanied by several CT transitions. This clearly reveals that the exciton chirality method cannot be applied here. This is fully compatible with our recent finding that the exciton chirality method fails to predict the AC of these donor–acceptor cyclophanes **1** or **2**.⁵ Previous examples that solely employed the exciton chirality method for determining the AC are therefore in ambiguity and remains to be elucidated more precisely.³⁹

Molecular orbitals of the three donor–acceptor cyclophanes **1–3** are quite similar to each other (but significantly different

from those of the non-CT cyclophane **4**), as can be seen from Figure 6. In short, the HOMO–1, HOMO, and LUMO+2 orbitals are located essentially on the donor moiety, while the HOMO–2, LUMO, and LUMO+1 orbitals on the acceptor for all three CT-cyclophanes. In contrast, these orbitals are equally located on both aromatic rings in the case of **4** (for the detailed transition properties of each systems, see Table S3 in Supporting Information). This clearly indicates that the orbital interactions between two aromatic planes are very small (see also Figure S5 in Supporting Information), and this situation can be further sustained by the Mulliken–Hush analysis (vide infra).

The most interesting features were found in the excited-state analysis of the non-CT cyclophane **4**. As can be seen in the bar-representation in Figure 5 (right), the bands at 230 nm (labeled b) and 300 nm (labeled a) exhibit apparent exciton couplings. These signals are obedient to the exciton chirality

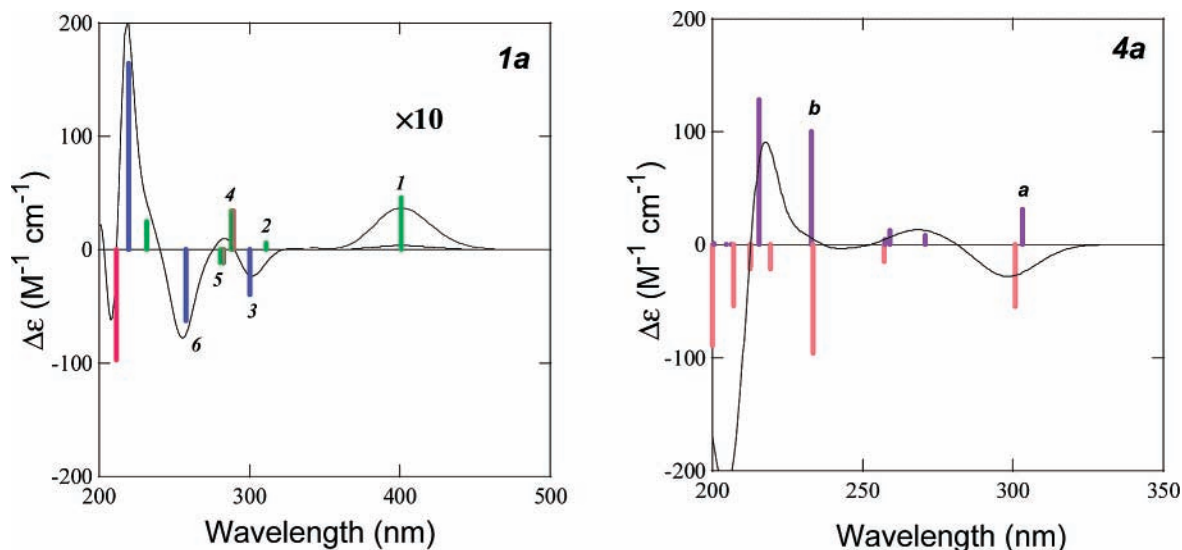


Figure 5. Simulated CD spectra and bar-representation of the excitation energies and rotatory strength of the transitions calculated at the BH-LYP/TZV2P level for the most abundant conformers **1a** and **4a**. The colors in **1a** code the character of the states as follows: green, donor to acceptor; blue, acceptor–acceptor; red, donor–donor transitions, respectively.

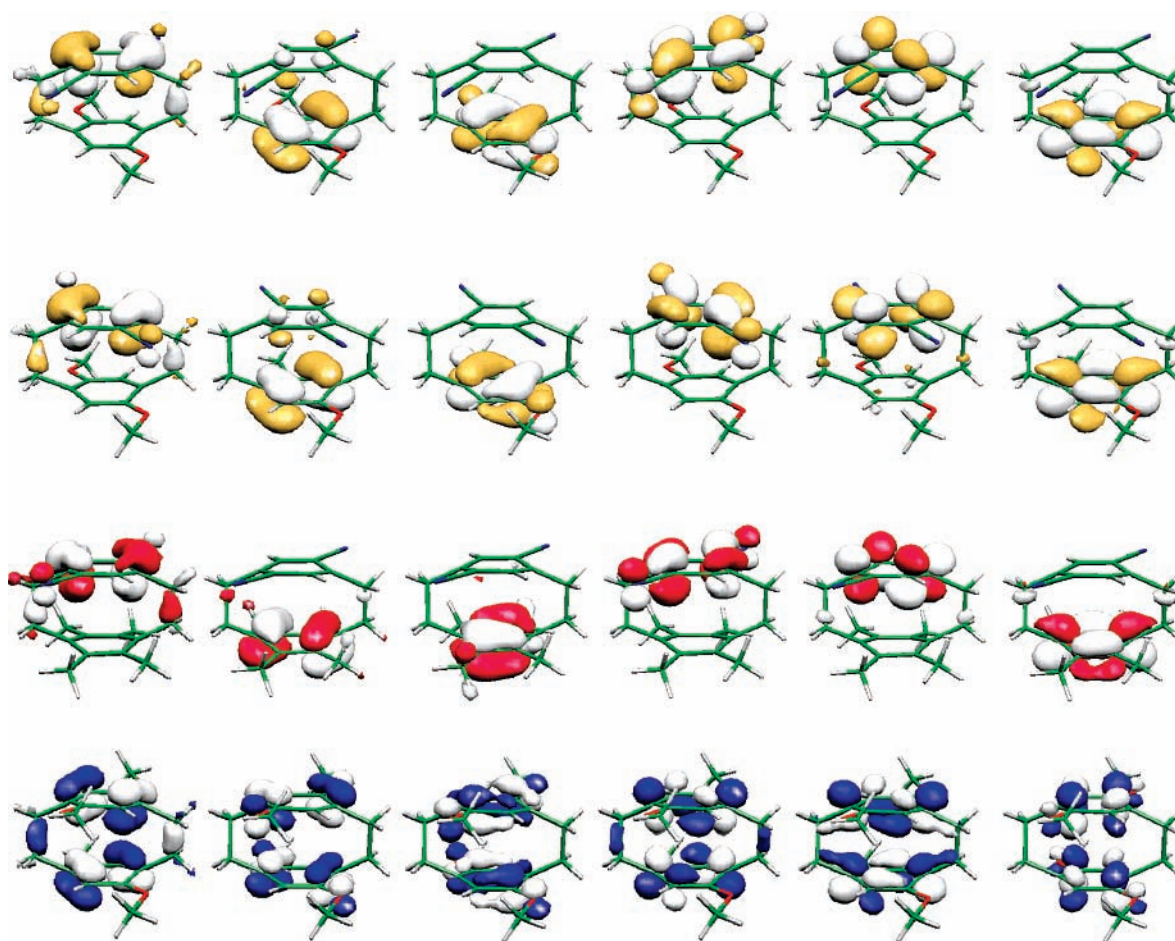


Figure 6. Molecular orbitals involved in the first five transitions of **1–4**. (nos. 82–87 for **1–3** and nos. 86–91 for **4**.) Note that the two images at the center of each row represent HOMO and LUMO orbitals.

theory applied to such paracyclophanes; i.e., the two couplings are opposite in sign and comparable in intensity (for further details, see Appendix S1 in Supporting Information). This behavior is completely predicted from the coupled transition moments of 2,5-dimethoxy-*p*-xylenes in the staggered orientation with an inter-ring distance of 3.2 Å. However, we note that the experimental CD spectrum observed for cyclophane **4**

does not exhibit such an exciton coupling pattern. As can be seen from Figure 5 (right), many of the transitions are closely located in energy and often opposite in sign, and therefore accumulated or cancelled out. Obviously, the spectrum obtained as a sum of the whole transitions does not represent the sign and magnitude of the original transitions, and hence, the AC determination of chiral cyclophanes (with or without donor–

TABLE 3: Summary of Photophysical Properties of Donor–acceptor Cyclophanes 1–3^a

	$r_{\text{DA}}, \text{\AA}$	$g = \Delta\epsilon/\epsilon$	$\lambda_{\text{CT}}, \text{nm}$	$\nu_{\text{CT}}, \text{cm}^{-1}$	$\Delta\nu_{1/2}, \text{cm}^{-1}$	$\epsilon_{\text{CT}}, \text{M}^{-1} \text{cm}^{-1}$	$Z (\%)$	$H_{\text{DA}}, \text{cm}^{-1}$
1	3.054	9.9×10^{-3}	423 ± 2	23600	1790 ± 80	49 ± 16	0.035	310 ± 60
2	3.036	1.4×10^{-3}	407 ± 3	24600	1870 ± 120	153 ± 100	0.107	570 ± 230
3	3.204	4.9×10^{-3}	380 ± 1	26300	1600 ± 10	118 ± 5	0.059	450 ± 10

^a $H_{\text{DA}} = 0.0206 (\nu_{\text{CT}} \Delta\nu_{1/2} \epsilon_{\text{CT}})^{1/2} / r_{\text{DA}}$. $Z = 2 c_b^2 = 1 - [1 - (2H_{\text{DA}}/\nu_{\text{CT}})^2]^{1/2}$. See ref 45.

acceptor interactions) by the conventional exciton chirality method is very controversial or even leads to erroneous conclusions. Therefore, the detailed analysis of the transitions by quantum chemical methods, such as TD–DFT calculation of the CD spectra, is strongly recommended for AC determinations.

Mulliken–Hush Analysis Applied to Donor–Acceptor Cyclophanes 1–3. The CT transition is known to reflect the electronic coupling element according to the relationship by Hush and co-workers:⁴⁰

$$H_{\text{ab}}(\text{cm}^{-1}) = 0.0206 \times \frac{\sqrt{\nu_{\text{CT}} \Delta\nu_{1/2} \epsilon_{\text{CT}}}}{r_{\text{DA}}}$$

where ν_{CT} and $\Delta\nu_{1/2}$ are the maximum and full width at half-height of the (deconvoluted) visible absorption band, ϵ_{CT} the molar extinction coefficient (in $\text{M}^{-1} \text{cm}^{-1}$) at the CT band maximum, and r_{DA} the effective separation of the donor and acceptor centers in the complex (in \AA). We took the r_{DA} values for **1** and **2** as the distances between the ring centers found in the X-ray structures, but for **3** the value from the DFT–D optimized geometry was used (Table 1). As shown in Table 3, the electronic coupling element H_{ab} calculated for the three donor–acceptor cyclophanes is in the range of 300–600 cm^{-1} , which is considerably smaller than those of known CT complexes.⁴¹ It should be noted that the H_{ab} value of the eclipsed **2** is 1.8 times larger than that of staggered form of **1**. Therefore, it is concluded that the overlap of the corresponding orbitals is also dependent on the molecular shape, as the transition energy and the bandwidth are essentially the same for **1** and **2**. The H_{ab} value for **3** is a result of compensation of having an electronically less-donating donor moiety and a better overlap of the donor–acceptor (compared to **1**). In all cases, the degree of charge transfer (Z) is very small or negligible (less than 0.1%). One interesting point to note is that the anisotropy factor ($g = \Delta\epsilon/\epsilon$) found in the experimental CD spectra becomes larger as the degree of charge transfer (H_{AD} or Z value) is decreased. When the degree of charge transfer becomes larger, the better overlap between donor and acceptor leads to the higher probability of the (electronic) CT transition (i.e.; larger ϵ_{CT}), eventually reducing the anisotropy factors.

Simulation of the CD Spectra of Intermolecular CT Model Systems. A Comparison with the CD Spectra of Related Paracyclophanes. In order to examine the effect of inter-ring distance and inter-ring twist angle on the calculated CD spectra, we examined a model system composed of 2,5-dicyanoxylylene and 2,5-dimethoxyxylylene shown in Chart 3. Note that the donor–acceptor geometry (with an angle of 0° and a distance of 3.1 \AA) is essentially the same as the parent paracyclopheane **1** except for the ring deformations. Intriguingly, the effect of deformation on the calculated CD spectra turned out to be small, since the CD spectrum calculated for this intermolecular CT complex reproduces most of the spectral patterns found in paracyclopheane **1** (see Figure S5, left, in the Supporting Information).⁴² This is in accordance with the results of other studies such as the harmonic oscillator model of aromaticity (HOMA)⁴³ and nucleus-independent chemical shift (NICS)⁴⁴

investigations, suggesting that the rings in [2.2]cyclophanes retain aromaticity, even though they are not completely planar and have alternant C–C bond lengths.

The effects of inter-ring distance and angle on the CD spectra are summarized in Figure 7. In general, the transitions are shifted by changing the donor acceptor distance, while no such shift is induced by changing the inter-ring angle. As the donor–acceptor distances decreases and thus the donor–acceptor interaction increases, the transition energies for the CT and the first π – π^* transitions gradually lower. The magnitude of the shift is smaller for the transitions in the shorter wavelength region. Most interestingly, the rotatory strength of the $^1\text{L}_b$ transition uniformly decreases with increasing inter-ring distance, while that of the CT transitions are more dramatically affected, showing a rapid decrease in intensity with a gradual bathochromic peak shift with accompanying switching of the sign from negative to positive at a distance of 3.5 \AA . Note that the representative equilibrium distance of intermolecular donor–acceptor complex is about 3.5 \AA .⁴⁶ This means that the Cotton effect(s) of the CT bands in such complexes are very weak, which is indeed the case.^{47,48}

The effect of the angle between the donor and acceptor groups on the CT-band Cotton effect is also impressive. Thus, the sign changes from negative to positive by changing the angle from -10° to $+10^\circ$, while the effect on the $^1\text{L}_b$ transitions is less dramatic. The sensitive nature of the sign and intensity of the Cotton effect at the CT band in donor–acceptor complexes may be applicable to the evaluation of conformational and configurational changes of relatively large molecules, if combined with the careful analysis by the quantum chemical studies.

4. Summary and Conclusions

This is the first comparative study of the experimental and simulated chiroptical properties of paracyclophanes with and without donor–acceptor interactions. Calculations of the optical rotations, vibrational and electronic CD spectra, as well as a qualitative analysis of the excited states were performed by the state-of-the-art quantum chemical methods. The major outcomes from this study are summarized as follows:

(1) The dispersion corrected DFT–D method with a basis-set of triple- ζ quality with an appropriate polarization functions successfully optimizes the geometries of donor–acceptor cyclophanes to give structures in excellent agreement with the X-ray crystallographic structures. The structures obtained can be used for further calculations of the chiroptical properties such as optical rotation and CD spectra of cyclophanes. The single-point SCS-MP2 energies calculated for these DFT–D optimized structures are suitable for the calculation of a reliable thermal population of the relevant conformers.

(2) The calculated specific rotations obtained at the BH-LYP/aug-cc-pVDZ level provide only qualitative information on the AC of the cyclophanes, as the absolute values significantly deviate from the experimental values. In addition, the computed rotations were found to be very sensitive to the ground-state geometries employed (DFT or MP2).

(3) The VCD spectra simulated at the B3-LYP/6-31G(d) level are not always consistent with the experimental data. Hence,

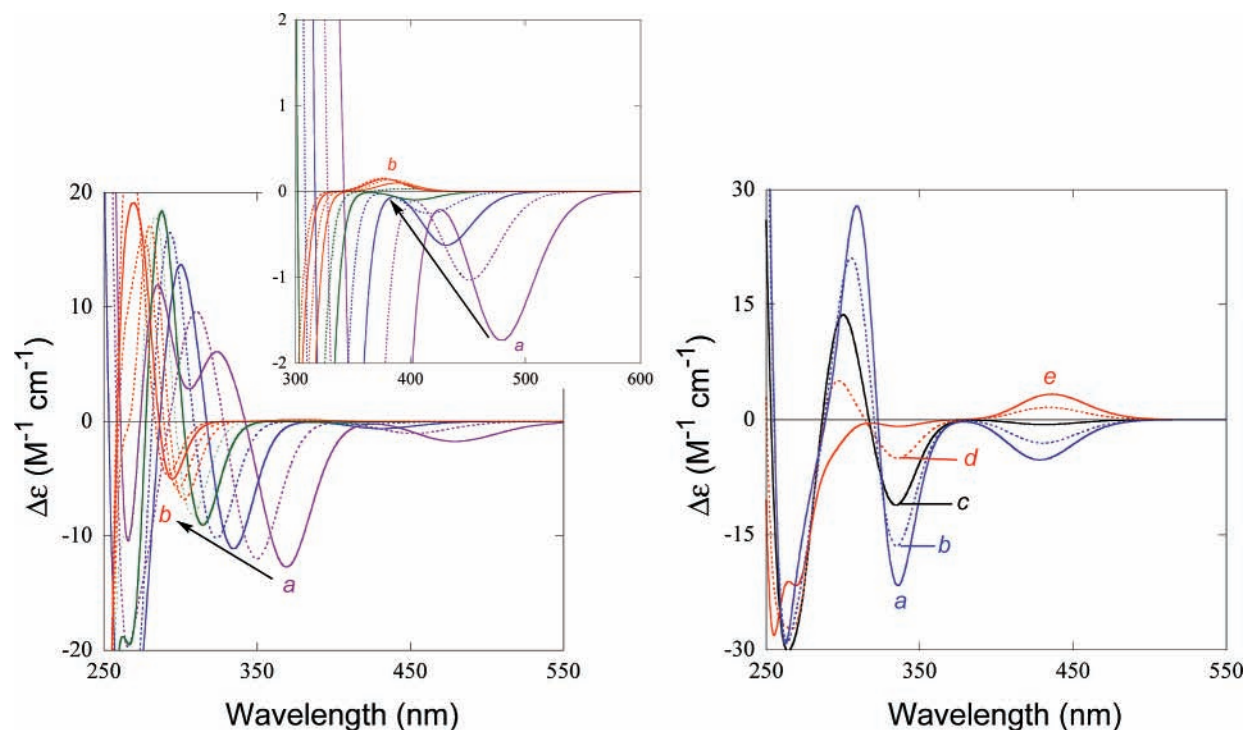
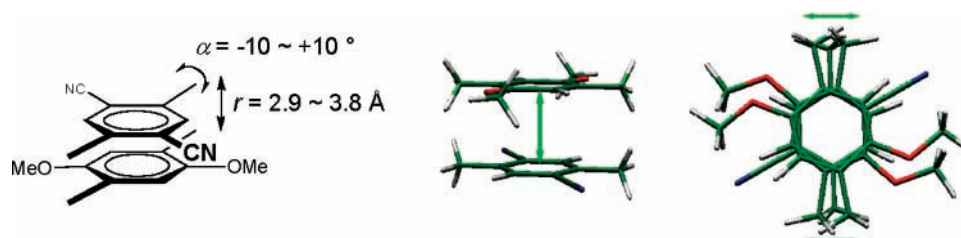


Figure 7. Calculations of CD spectra of model CT complexes. Left: Effect of inter-plane distance on the circular dichroism of the donor–acceptor system. The distance is incrementally (step = 0.1 Å) shifted from (a) 2.9 to (b) 3.8 Å. Inset: Expansion of the CT band region. Right: Effect of inter-ring rotation angle on the circular dichroism of the donor–acceptor system. The angle is incrementally shifted from (a) -10° , (b) -5° , (c) $\pm 0^\circ$, (d) $+5^\circ$, and (e) $+10^\circ$ with a constant inter-plane distance (3.1 Å). All spectra were shifted by 0.2 eV to the red.

CHART 3: Structure of Model CT Complexes



one should be cautious in assigning the AC of chiral cyclophanes by comparing the theoretical and experimental VCD spectra, since the disagreement in signal intensity and pattern is often observed in several transitions. Nevertheless, for the VCD bands that have mirror images for the enantiomers, the agreement between theoretical and experimental VCD signs appears to be sufficient enough to suggest the absolute configuration.

(4) The experimental CD spectra of donor–acceptor cyclophanes **1** and **2** are very well reproduced with the BH-LYP functional which contains 50% exact exchange. The analysis of the configuration contributions showed that the observed CD spectra essentially result from a simple overlap of the Cotton effects of pure π – π^* transitions in the donor or acceptor part as well as the CT transitions. Thus, the exciton chirality method cannot be applied to the AC determination.

(5) The Mulliken–Hush and molecular orbital analysis revealed that the interactions between the donor and the acceptor moieties in CT cyclophanes **1**–**3** are very small. The intensity of the observed Cotton effect at the CT band (*g* factor) is affected by the degree of charge transfer.

(6) The experimental CD spectrum of more congested CT-cyclophane **3** was reproduced in a less satisfactory manner compared to the cases of **1** and **2**, but the AC was safely determined by a comparison of theoretical and experimental

data. The CD spectrum of **3** was reproduced very well with the more sophisticated RI-CC2 calculation.

(7) The calculation also revealed that exciton couplings are involved indeed in non-CT cyclophane **4**. However, care must be taken in applying the exciton chirality method to the observed CD spectra even in such a case, since a complicated cancellation of the transitions may conceal the real exciton coupling in the observed spectrum.

(8) From the examinations of possible Cotton effects in an intermolecular donor–acceptor model system, we have demonstrated that both the inter-ring distance and the inter-ring twisting angle more critically affect the CT transition than the 1L_b transition. It is also a crucial finding that the Cotton effect of the CT band becomes almost zero at an inter-ring distance of 3.5 Å, which incidentally coincides with the equilibrium distance of many CT complexes. Hence, one should be very cautious in analyzing the experimental CD of CT bands.

In summary, efficient TD–DFT calculations of the chiral donor–acceptor cyclophanes reproduce the experimental CD spectra quite accurately by using the BH-LYP functional with basis sets of triple- ζ quality with proper polarization functions. For the AC assignment of cyclophanes and related molecules, the combination of experimental and BH-LYP calculated CD spectra is the only reasonable choice, which is superior to the

well-documented specific rotation or VCD-based methods in terms of the accuracy, the computational costs, and, more importantly, the amount of required enantiopure samples for experimental measurements.

Acknowledgment. T.M. thanks the Alexander von Humboldt-Stiftung for the fellowship. Financial support of this work by a Grant-in-Aid for Scientific Research from the Ministry of Education, Culture, Sports, Science, and Technology of Japan to T.M. is gratefully acknowledged. We thank Mr. Takahiro Furo for preliminary calculation on VCD spectra. We also thank Profs. Nobuyuki Harada and Thorsten Bach and Drs. Christian Mück-Lichtenfeld, Christian Diedrich, and Manuel Piacenza for fruitful discussion.

Supporting Information Available: Text, including tables and figures, giving general experimental details, complete refs 7 and 17, conditions of chiral HPLC (Table S1), summary of experimental CD spectra of **1–4** (Table S2), comparison of DFT and X-ray structures of **1** and **2** (Figure S1), calculated CD spectra of each conformers of **1**, **2**, and **4** (Figure S2), effects of functional and basis-set on the calculated CD spectra of **3** (Figure S3), bar representation of calculated CD spectra of **1a–4a** (Figure S4), excited-state analysis of **1–4** (Table S3), energy levels of molecular orbitals of **1–4** (Figure S5), molecular orbitals of the reference molecules (Figure S6), comparison of the calculated CD spectra of cyclophanes and CT complexes (Figure S7), theoretical application of the exciton coupling theory on the cyclophane **4** (Appendix S1), and Cartesian coordinates of the optimized geometries of the conformations of cyclophanes (**1–4**). This material is available free of charge via the Internet at <http://pubs.acs.org>.

References and Notes

- (1) (a) Gleiter, R.; Hopf, H., Eds. *Modern Cyclophane Chemistry*; Wiley-VCH: Weinheim, Germany, 2004. (b) Vögtle, F. *Cyclophane Chemistry*; Wiley: New York, 1993. (c) Diederich, F. *Cyclophanes: Monographs in Supramolecular Chemistry*; The Royal Society of Chemistry: London, 1991. (d) Keehn, P. M.; Rosenfeld, S. M., Eds. *Cyclophanes*; Academic Press: New York, 1983.
- (2) (a) Gibson, S. E.; Knight, J. D. *Org. Biomol. Chem.* **2003**, *1*, 1256–1269. (b) Ma, Y.; Song, C.; Ma, C.; Sun, Z.; Chai, Q.; Andrus, M. B. *Angew. Chem., Int. Ed.* **2003**, *42*, 5871–5874. (c) Sato, I.; Ohno, A.; Aoyama, Y.; Kasahara, T.; Soai, K. *Org. Biomol. Chem.* **2003**, *1*, 244–246. (d) Zanotti-Gerosa, A.; Malan, C.; Herzberg, D. *Org. Lett.* **2001**, *3*, 3687–3690.
- (3) Harada, N.; Nakanishi, K. *Circular Dichroic Spectroscopy. Exciton Coupling in Organic Stereochemistry*; University Science Books: Mill Valley, CA, 1983.
- (4) (a) Lanari, D.; Marocchi, A.; Minuti, L.; Rosini, C.; Superchi, S.; Taticchi, A. *Tetrahedron: Asymmetry* **2002**, *13*, 1257–1263. (b) Rosini, C.; Ruzziconi, R.; Superchi, S.; Fringuelli, F.; Piermatti, O. *Tetrahedron: Asymmetry* **1998**, *9*, 55–62.
- (5) Furo, T.; Mori, T.; Wada, T.; Inoue, Y. *J. Am. Chem. Soc.* **2005**, *127*, 8242–8243, 16338.
- (6) Recent reviews: (a) Grimme, S. *Rev. Comput. Chem.* **2004**, *20*, 153–218. (b) Dreuw, A.; Head-Gordon, M. *Chem. Rev.* **2005**, *105*, 4009–4037. (c) Polavarapu, P. L. *Chirality* **2002**, *14*, 768–781.
- (7) *TURBOMOLE, version 5.6*, Ahlrichs, R. et al.; Universität Karlsruhe: Karlsruhe, 2003. See also: <http://www.cosmologic.de/turbomole.html>.
- (8) (a) Eichkorn, K.; Treutler, O.; Öhm, H.; Häser, M.; Ahlrichs, R. *Chem. Phys. Lett.* **1995**, *240*, 283–289. (b) Weigend, F.; Häser, M. *Theor. Chem. Acc.* **1997**, *97*, 331–340. (c) Grimme, S.; Waletzke, M. *Phys. Chem. Chem. Phys.* **2000**, *2*, 2075–2081. (d) Vahtras, O.; Almlöf, J.; Feyereisen, M. W. *Chem. Phys. Lett.* **1993**, *213*, 514–518.
- (9) Hättig, C.; Weigend, F. *J. Chem. Phys.* **2000**, *113*, 5154–5161.
- (10) Bauernschmidt, R.; Ahlrichs, R. *Chem. Phys. Lett.* **1996**, *256*, 454–464.
- (11) Grimme, S. *J. Comput. Chem.* **2004**, *25*, 1463–1473.
- (12) (a) Grimme, S. *J. Phys. Chem. A* **2005**, *109*, 3067–3077. (b) Goumans, T. P. M.; Ehlers, A. W.; Lammertsma, K.; Würthwein, E.-U.; Grimme, S. *Chem.—Eur. J.* **2004**, *10*, 6468–6475. (c) Grimme, S. *J. Chem. Phys.* **2003**, *118*, 9095–9102.
- (13) Schäfer, A.; Huber, C.; Ahlrichs, R. *J. Chem. Phys.* **1994**, *100*, 5829–5835.
- (14) Schäfer, A.; Horn, H.; Ahlrichs, R. *J. Chem. Phys.* **1992**, *97*, 2571–2577.
- (15) (a) Diedrich, C.; Grimme, S. *J. Phys. Chem. A* **2003**, *107*, 2524–2539. (b) Autschbach, J.; Ziegler, T.; van Gisbergen, S. J. A.; Baerends, E. J. *J. Chem. Phys.* **2002**, *116*, 6930–6940.
- (16) Christiansen, O.; Koch, H.; Jörgensen, P. *Chem. Phys. Lett.* **1995**, *243*, 409–418.
- (17) *Gaussian 03, Revision B.03*; Frisch, M. J.; et al. Gaussian, Inc.: Wallingford, CT, 2004.
- (18) (a) Mori, T.; Izumi, H.; Inoue, Y. *J. Phys. Chem. A* **2004**, *108*, 9540–9549. (b) Izumi, H.; Yamagami, S.; Futamura, S.; Nafie, L. A.; Dukor, R. K. *J. Am. Chem. Soc.* **2004**, *126*, 194–198. (c) Wang, F.; Polavarapu, P. L.; *J. Phys. Chem. A* **2000**, *104*, 1822–1826.
- (19) For recent investigations, see: (a) Pelloni, S.; Lazzaretto, P.; Zanasi, R. *J. Phys. Chem. A* **2007**, *111*, 3110–3123. (b) Frontera, A.; Quinonero, D.; Garau, C.; Costa, A.; Ballester, P.; Deyà, P. M. *J. Phys. Chem. A* **2006**, *110*, 5144–5148. (c) Poater, J.; Bofill, J. M.; Alemany, P.; Solà, M. *J. Org. Chem.* **2006**, *71*, 1700–1702. (d) Amthor, S.; Lambert, C. *J. Phys. Chem. A* **2006**, *110*, 3495–3504. (e) Amthor, S.; Lambert, C. *J. Phys. Chem. A* **2006**, *110*, 1177–1189. (f) Gibson, S. E.; Knight, J. D. *Org. Biomol. Chem.* **2003**, *1*, 1256–1269. (g) de Meijere, A.; König, B. *Synlett* **1997**, 1221–1232.
- (20) (a) Grimme, S. *Chem.—Eur. J.* **2004**, *10*, 3423–3429. See, on the contrary: (b) Caramori, G. F.; Galembeck, S. E. *J. Phys. Chem. A* **2007**, *111*, 1705–1712. (c) Caramori, G. F.; Galembeck, S. E.; Laali, K. K. *J. Org. Chem.* **2005**, *70*, 3242–3250.
- (21) (a) Grimme, S.; Diedrich, C.; Korth, M. *Angew. Chem., Int. Ed.* **2006**, *45*, 625–629. (b) Piacenza, M.; Grimme, S. *J. Am. Chem. Soc.* **2005**, *127*, 14841–14848. (c) Piacenza, M.; Grimme, S. *Chem. Phys. Chem.* **2005**, *6*, 1554–1558.
- (22) Parac, M.; Etinski, M.; Peric, M.; Grimme, S. *J. Chem. Theory Comput.* **2005**, *1*, 1110–1118.
- (23) Grimme, S.; Antony, J.; Schwabe, T.; Mück-Lichtenfeld, C. *Org. Bio. Chem.* **2007**, *5*, 741–758.
- (24) (a) Grimme, S. *J. Phys. Chem. A* **2005**, *109*, 3067–3077. (b) Goumans, T. P. M.; Ehlers, A. W.; Lammertsma, K.; Würthwein, E.-U.; Grimme, S. *Chem.—Eur. J.* **2004**, *10*, 6468–6475. (c) Grimme, S. *J. Chem. Phys.* **2003**, *118*, 9095–9102.
- (25) (a) Sinnokrot, M. O.; Valeev, W. F.; Sherrill, C. D. *J. Am. Chem. Soc.* **2002**, *124*, 10887–10893. (b) Henseler, D.; Hohlneicher, G. *J. Phys. Chem. A* **1998**, *102*, 10828–10833. (c) Walden, S. E.; Glatzhofer, D. T. *J. Phys. Chem. A* **1997**, *101*, 8233–8241. (d) Hope, H.; Bernstein, J.; Trueblood, K. N. *Acta Crystallogr.* **1972**, *B28*, 1733–1743.
- (26) (a) Grimme, S.; Furche, F.; Ahlrichs, R. *Chem. Phys. Lett.* **2002**, *361*, 321–328. (b) Grimme, S. *Chem. Phys. Lett.* **2001**, *339*, 380–388. (c) Ruud, K.; Helgaker, T. *Chem. Phys. Lett.* **2002**, *352*, 533–539. (d) Autschbach, J.; Patchkovskii, S.; Ziegler, T.; van Gisbergen, S. J. A.; Baerends, E. J. *J. Chem. Phys.* **2002**, *117*, 581–592. (e) Stephens, P. J.; Devlin, F. J.; Cheeseman, J. R.; Frisch, M. J. *J. Phys. Chem. A* **2001**, *105*, 5356–5379.
- (27) (a) Diedrich, C.; Grimme, S. *J. Phys. Chem. A* **2003**, *107*, 2524–2539. (b) Autschbach, J.; Ziegler, T.; van Gisbergen, S. J. A.; Baerends, E. J. *J. Chem. Phys.* **2002**, *116*, 6930–6940.
- (28) (a) Furche, F.; Ahlrichs, R.; Wachsmann, C.; Weber, E.; Sobanski, A.; Vögtle, F.; Grimme, S. *J. Am. Chem. Soc.* **2000**, *122*, 1717–1724. (b) Autschbach, J.; Ziegler, T.; van Gisbergen, S. J. A.; Baerends, E. J. *J. Chem. Phys.* **2002**, *116*, 6930–6940. (c) Pecul, M.; Ruud, K.; Helgaker, T. *Chem. Phys. Lett.* **2004**, *388*, 110–119.
- (29) (a) Dunning, T. H. *J. Chem. Phys.* **1993**, *98*, 7059–7071. (b) Kendall, R. A.; Dunning, T. H.; Harrison, R. J. *J. Chem. Phys.* **1992**, *96*, 6796–6806.
- (30) (a) Dreuw, A.; Fleming, G. R.; Head-Gordon, M. *J. Phys. Chem. B* **2003**, *107*, 6500–6503. (b) Tozer, D. J.; Amos, R. D.; Handy, N. C.; Roos, B. J.; Serrano-Andres, L. *Mol. Phys.* **1999**, *97*, 859–868. (c) Sobolewski, A. L.; Domcke, W. *Chem. Phys.* **2003**, *294*, 73–83. (d) Dreuw, A.; Head-Gordon, M. *J. Am. Chem. Soc.* **2004**, *126*, 4007–4016. (e) Dreuw, A.; Weisman, J. L.; Head-Gordon, M. *J. Chem. Phys.* **2003**, *119*, 2943–2946. (f) van Mourik, T.; Karamertzanis, P. G.; Price, S. L. *J. Phys. Chem. A* **2006**, *110*, 8–12.
- (31) (a) Shin, S.; Nakata, M.; Hamada, Y. *J. Phys. Chem. A* **2006**, *110*, 2122–2129. (b) Monde, K.; Taniguchi, T.; Miura, N.; Nishimura, S.-I. *J. Am. Chem. Soc.* **2004**, *126*, 9496–9497. (c) Schweitzer-Stenner, R.; Eker, F.; Griebenow, K.; Cao, X.; Nafie, L. A. *J. Am. Chem. Soc.* **2004**, *126*, 2768–2776.
- (32) (a) Fristrup, P.; Lassen, P. R.; Johannessen, C.; Tanner, D.; Norby, P.-O.; Jalkanen, K. J.; Hemmingsen, L. *J. Phys. Chem. A* **2006**, *110*, 9123–9129. (b) Carosati, E.; Cruciani, G.; Chiarini, A.; Budriesi, R.; Ioan, P.; Spisani, R.; Spinelli, D.; Cosimelli, B.; Fusi, F.; Frosini, M.; Matucci, R.; Gasparrini, F.; Ciogli, A.; Stephens, P. J.; Devlin, F. J. *J. Med. Chem.* **2006**, *49*, 5206–5216. (c) Tarczay, G.; Magyarfalvi, G.; Vass, E. *Angew. Chem., Int. Ed.* **2006**, *45*, 1775–1777. (d) Brotin, T.; Cavagnat, D.; Dutasta, J.-P.;

- Buffeteau, T. *J. Am. Chem. Soc.* **2006**, *128*, 5533–5540. (e) Monde, K.; Taniguchi, T.; Miura, N.; Vairappan, C. S.; Suzuki, M. *Chirality* **2006**, *18*, 335–339. (f) Naubron, J.-V.; Giordano, L.; Fotiadu, F.; Buergi, T.; Vanthuyne, N.; Roussel, C.; Buono, G. *J. Org. Chem.* **2006**, *71*, 5586–5593. (g) Devlin, F. J.; Stephens, P. J.; Besse, P. *J. Org. Chem.* **2005**, *70*, 2980–2993. (h) Devlin, F. J.; Stephens, P. J.; Besse, P. *Tetrahedron Asym.* **2005**, *16*, 1557–1566. (i) Devlin, F. J.; Stephens, P. J.; Bortolini, O. *Tetrahedron Asym.* **2005**, *16*, 2653–2663. (j) Kuppens, T.; Vanduyck, K.; Van der Eycken, J.; Herrebout, W.; van der Veken, B. J.; Bultinck, P. *J. Org. Chem.* **2005**, *70*, 9103–9114. (k) He, J.; Petrovich, A.; Polavarapu, P. L. *J. Phys. Chem. A* **2004**, *108*, 1671–1680. (l) Devlin, F. J.; Stephens, P. J.; Scafato, P.; Superchi, S.; Rosini, C. *Chirality* **2002**, *14*, 400–406. (m) Devlin, F. J.; Stephens, P. J.; Oesterle, C.; Wiberg, K. B.; Cheeseman, J. R.; Frisch, M. J. *J. Org. Chem.* **2002**, *67*, 8090–8096. (n) Stephens, P. J.; Devlin, F. J.; Aamouche, A. *ACS Symp. Ser.* **2002**, *810*, 18–33. (o) Aamouche, A.; Devlin, F. J.; Stephens, P. J. *J. Am. Chem. Soc.* **2000**, *122*, 2346–2354.
- (33) (a) Tam, M. C.; Crawford, T. D. *J. Phys. Chem. A* **2006**, *110*, 2290–2298. (b) Stephens, P. J.; McCann, D. M.; Devlin, F. J.; Cheeseman, J. R.; Frisch, M. J. *J. Am. Chem. Soc.* **2004**, *126*, 7514–7521.
- (34) (a) McCann, D. M.; Stephens, P. J.; Cheeseman, J. R. *J. Org. Chem.* **2004**, *69*, 8709–8717. (b) Autschbach, J.; Jensen, L.; Schatz, G. C.; Tse, Y. C. E.; Krykunov, M. *J. Phys. Chem. A* **2006**, *110*, 2461–2473. (c) Kundrat, M. D.; Autschbach, J. *J. Phys. Chem. A* **2006**, *110*, 12908–12917.
- (35) Notations from Gaussian package corresponds to: BH&HLYP. See also: (a) Maity, D. K.; Duncan, W. T.; Truong, T. N. *J. Phys. Chem. A* **1999**, *103*, 2152–2159. (b) Duncan, W. T.; Truong, T. N. *J. Chem. Phys.* **1995**, *103*, 9642–9652.
- (36) Mori, T.; Inoue, Y.; Grimme, S. *J. Org. Chem.* **2006**, *71*, 9797–9806. See also, Mori, T.; Inoue, Y.; Grimme, S. *J. Phys. Chem. A* **2007**, *111*, 4222–4234.
- (37) (a) Dreuw, A.; Fleming, G. R.; Head-Gordon, M. *J. Phys. Chem. B* **2003**, *107*, 6500–6503. (b) Tozer, D. J.; Amos, R. D.; Handy, N. C.; Roos, B. J.; Serrano-Andres, L. *Mol. Phys.* **1999**, *97*, 859–868. (c) Sobolewski, A. L.; Domcke, W. *Chem. Phys.* **2003**, *294*, 73–83.
- (38) Considering the complexity of this CD spectrum, the agreement can be regarded as very good and slight deviations around 300 nm between the theory and the experiment can be tolerated.
- (39) (a) Gawronfiski, J.; Grajewski, J.; Drabowicz, J.; Mikołajczyk, M. *J. Org. Chem.* **2003**, *68*, 9821–9822. (b) Gawronfiski, J.; Gawrofiska, K.; Brzostowska, M. *Tetrahedron Lett.* **1999**, *40*, 1191–1194.
- (40) (a) Marcus, R. A.; Sutin, N. *Biochim. Biophys. Acta* **1985**, *811*, 265–322. (b) Hush, N. S. *Coord. Chem. Rev.* **1985**, *64*, 135–157. (c) Hush, N. S. *Electrochim. Acta* **1968**, *13*, 1005–1023. (d) Hush, N. S. *Prog. Inorg. Chem.* **1967**, *8*, 391–444. (e) Hush, N. S. *Trans. Faraday Soc.* **1961**, *57*, 557–580.
- (41) (a) Sun, D.-L.; Rosokha, S. V.; Lindeman, S. V.; Kochi, J. K. *J. Am. Chem. Soc.* **2003**, *125*, 15950–15963. (b) Lindeman, S. V.; Hecht, J.; Kochi, J. K. *J. Am. Chem. Soc.* **2003**, *125*, 11597–11606. (c) Lindeman, S. V.; Rosokha, S. V.; Sun, D.; Kochi, J. K. *J. Am. Chem. Soc.* **2002**, *124*, 843–855.
- (42) Note that the apparently missing CT transition in the model system is due to the slightly shorter (effective) distances in the corresponding paracyclophanes. It is also to note that the calculated CD spectra of the model for the eclipsed cyclophane **2** differ considerably from the experimental spectra.
- (43) (a) Kruszewski, J.; Krygowski, T. M. *Tetrahedron Lett.* **1972**, *13*, 3839–3842. (b) Krygowski, T. M. *J. Chem. Inf. Comput. Sci.* **1993**, *33*, 70–78.
- (44) (a) Schleyer, P. v. R.; Maerker, C.; Dransfeld, A.; Jiao, H.; Hommes, N. J. R. v. E. *J. Am. Chem. Soc.* **1996**, *118*, 6317–6318. (b) Schleyer, P. v. R. *Chem. Rev.* **2005**, *105*, 3433–3435.
- (45) Gwaltney, S. R.; Rosokha, S. V.; Head-Gordon, M.; Kochi, J. K. *J. Am. Chem. Soc.* **2003**, *125*, 3273–3283.
- (46) (a) Yoshikawa, H.; Nishikiori, S.-i.; Ishida, T. *J. Phys. Chem. B* **2003**, *107*, 9261–9267. (b) Liao, M.-S.; Lu, Y.; Scheiner, S. *J. Comput. Chem.* **2003**, *24*, 623–631.
- (47) (a) Briegleb, G.; Kuballe, H. G. *Angew. Chem., Int. Ed. Engl.* **1964**, *3*, 307–308. (b) Briegleb, G.; Kuballe, H. G.; Henschel, K. *J. Phys. Chem. (Frankfurt)* **1965**, *46*, 229–249. (c) Briegleb, G.; Kuballe, H. G.; Henschel, K.; Euing, W. *Ber. Bunsen-Ges. Phys. Chem.* **1972**, *76*, 101–105. (d) Geissler, U.; Schulz, R. C. *Makromol. Chem., Rapid Commun.* **1981**, *2*, 591–594.
- (48) (a) Mori, T.; Inoue, Y. *Angew. Chem., Int. Ed.* **2006**, *44*, 2582–2585. (b) Mori, T.; Ko, Y. H.; Kim, K.; Inoue, Y. *J. Org. Chem.* **2006**, *71*, 3232–3247.